Editors' Suggestion

# Magnetochiral Dichroism in a Collinear Antiferromagnet with No Magnetization

Tatsuki Sato,[1] Nobuyuki Abe,[1] Shojiro Kimura,[2] Yusuke Tokunaga,[1] and Taka-hisa Arima[1]
[1]Department of Advanced Materials Science, University of Tokyo, Kashiwa 277-8561, Japan
[2]Institute for Materials Research, Tohoku University, Sendai 980-8577, Japan

(Received 4 January 2020; accepted 30 April 2020; published 27 May 2020)

We show the directional dichroism in a collinear antiferromagnet $MnTiO_3$. The dichroism between two distinctive antiferromagnetic states with opposite signs of staggered magnetic moments can be regarded as magnetochiral dichroism in the absence of external fields. Electric-field reversal of antiferromagnetic domain causes a change in the absorption intensity of unpolarized light around 2.15 eV. The difference in optical absorption between two antiferromagnetic states is reversed for the light propagating in the opposite direction. The absorption coefficient displays a hysteretic behavior for a cycle of sweeping the external electric or magnetic field.

DOI: 10.1103/PhysRevLett.124.217402

Symmetry breaking induces specific optical effects. The lack of rotation, mirror reflection, and time-reversal symmetries induce the linear dichroism, natural circular dichroism, and magnetic circular dichroism, respectively. For unpolarized light, the simultaneous violation of the spatial-inversion and time-reversal symmetries brings about nonreciprocal directional dichroism. Directional dichroism of unpolarized light was uncovered as the magnetochiral dichroism (MCHD) in 1998 [1] following the earlier theoretical prediction [2] and formulation [3,4].

The microscopic origin of MCHD is traceable to the interference between electric-dipole ($E1$) and magnetic-dipole ($M1$) transitions or between the $E1$ and electric-quadrupole ($E2$) transitions [4,5]. When the light of angular frequency $\omega$ propagates along the $z$ axis, the contribution of the $E1$–$M1$ interference to the absorbance is expressed as

$$\alpha^{E1-M1}(\omega) \propto \omega \mathrm{Im}[a_{xy}(\omega) - a_{yx}(\omega)]. \quad (1)$$

$a_{\alpha\beta}(\omega)$ represents dynamic linear magnetoelectric (ME) coupling where an oscillating magnetic field $\boldsymbol{B}(\omega)$ induces oscillating electric polarization $\boldsymbol{P}(\omega)$ as $P_\alpha(\omega) = a_{\alpha\beta}(\omega)B_\beta(\omega)$. Equation (1) says that MCHD arises in a material hosting the off-diagonal antisymmetric ME coupling, which is identified with magnetic toroidal moment $\boldsymbol{T}$ as $b(\omega)T^\mu = \varepsilon_{\mu\nu\lambda}a_{\nu\lambda}(\omega)$ with a function $b(\omega)$ of $\omega$ and the Levi-Civita symbol $\varepsilon_{ijk}$ [6]. In chiral materials, the toroidal moment $\boldsymbol{T}$ can be induced in proportion to magnetization $\boldsymbol{M}$. So far it has been established that net magnetization causes MCHD in various chiral magnets, such as ferromagnets [7], weak ferromagnets [8], and helimagnets in the magnetic field [9] when the light propagates along $\boldsymbol{M}$ and hence $\boldsymbol{T}$.

Motivated by recent developments in the field of antiferromagnetic spintronics [10–12], we pursue engineering of the dichroism in antiferromagnetic insulators. While antiferromagnets have no net magnetization, ordering of staggered moment $\boldsymbol{L}$ may break time reversal and spatial-inversion symmetries if a crystallographic unit cell contains pairs of magnetic ions connected by the space-inversion operation. A linear-ME antiferromagnet is an ideal platform for the MCHD of $\boldsymbol{L}$ origin, if an antisymmetric linear-ME coupling is activated by $\boldsymbol{L}$. Furthermore, one can also align the direction of $\boldsymbol{L}$ through the ME coupling, which is essential for the detection of directional dichroism in a macroscopic scale. In spite of possible novel functionalities, such as electric-field switching of color and optical imaging of antiferromagnetic domain patterns, directional dichroism in linear-ME antiferromagnets has been studied only in the terahertz range [13] and research for visible lights seems lacking.

Here we present the dichroism in a collinear antiferromagnet $MnTiO_3$. The asymmetry in the absorption coefficient for two distinctive antiferromagnetic states with opposite signs of $\boldsymbol{L}$ is observed. Furthermore, each antiferromagnetic state shows directional dichroism, which can be regarded as MCHD from symmetry consideration. $MnTiO_3$ crystallizes in the ilmenite structure with the centrosymmetric space group $R\bar{3}$ [14]. Buckled honeycomb layers of $Mn^{2+}$ with $S = 5/2$ and those of nonmagnetic $Ti^{4+}$ alternately stack along the $c$ axis [Fig. 1(a)]. In each honeycomb layer, inversion centers are located at the bond centers, but not at the atomic sites [Fig. 1(b)]. At Néel temperature $T_N = 65$ K, $MnTiO_3$ undergoes a magnetic phase transition. Antiferromagnetic honeycomb layers of $Mn^{2+}$ with the easy-axis anisotropy stack without doubling the unit cell [Fig. 1(a)] [15,16]. The $\boldsymbol{q} = \boldsymbol{0}$ antiferromagnetic ordering with electron spins of opposite orientations on each sublattice violates the time-reversal and spatial-inversion symmetries as in $Cr_2O_3$ [17]. The magnetic point group becomes $\bar{3}'$, which hosts the linear-ME tensor $a$ represented as

 

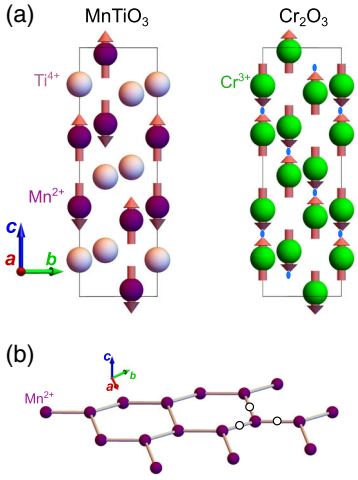


FIG. 1. (a) Antiferromagnetic structures of $MnTiO_3$ (left) and $Cr_2O_3$ (right) projected along the $a$ axis. Arrows denote magnetic moments. Purple, light-purple and green spheres denote $Mn^{2+}$, $Ti^{4+}$, and $Cr^{3+}$ ions, respectively. Oxygen atoms are omitted. On the right panel, twofold rotation axes along the $a$ axis are denoted by blue symbols. (b) A honeycomb network of $Mn^{2+}$ in $MnTiO_3$. White circles denote inversion centers located at bond centers.

$$a \equiv \begin{pmatrix} a_\perp & a_t & 0 \\ -a_t & a_\perp & 0 \\ 0 & 0 & a_\parallel \end{pmatrix}, \tag{2}$$

with nonzero toroidal moment $T^c \propto a_t$ [18]. Note that the antisymmetric off-diagonal term $a_t$ in Eq. (2) is forbidden in linear-ME $Cr_2O_3$ of the corundum structure with twofold rotation axes along the $a$ axis as depicted in Fig. 1(a) [17]. Layered ordering of $Mn^{2+}$ and $Ti^{4+}$ is crucial to activate $T^c$. The presence of $a_t$, or toroidal moment $\boldsymbol{T} \| \boldsymbol{c}$, is associated with the lack of twofold symmetry in the ilmenite structure. In general, the sign of each component of linear-ME tensor $a$ in an antiferromagnet corresponds to the sign of the staggered moment. The free-energy component $\Delta\mathcal{F}$ related with the ME effect is represented as

$$\Delta\mathcal{F} = -c_\parallel L_c E_c H_c, \tag{3}$$

where $c_\parallel > 0$ is defined as $a_\parallel = c_\parallel L_c$ [18]. In $MnTiO_3$, $L_c$ is the difference between the magnetic moment on two distinct antiferromagnetic sublattices, left-handed and right-handed $MnO_6$ clusters (shown later). $E_c$ and $H_c$ are the electric and magnetic fields along the $c$ axis. In a static magnetic field $H_c > 0$, positive electric field $E_c > 0$ favors the $L_c > 0$ state, and $E_c < 0$ favors $L_c < 0$. When the energy barrier between the $L_c > 0$ and $L_c < 0$ states is small enough, we can isothermally flip $L_c$ by sweeping $E_c$ in a static $H_c$. Similarly, $L_c$ is also manipulated by sweeping $H_c$ in a static $E_c$. In this way, $L_c$ in $MnTiO_3$ is reversible by a combination of $E_c$ and $H_c$. In $MnTiO_3$, both $\boldsymbol{T}$ and $\boldsymbol{L}$ have the same symmetry, i.e., odd to spatial inversion and time reversal, and oriented along the $c$ axis. Therefore, $T^c$ should be expanded by odd powers of $L_c$ as $T^c = a_1 L_c + a_3 L_c^3 + \cdots$. Hence a combination of $E_c$ and $H_c$ can switch the toroidal moment $\boldsymbol{T}$ in $MnTiO_3$, as a magnetic field does the magnetization in a ferromagnet.

Single crystals of $MnTiO_3$ were grown by the floating-zone technique in Ar flow [18]. Temperature ($T$), magnetic-field ($H$), and electric-field ($E$) dependence change in electric polarization ($P$) was obtained by integrating the displacement current with respect to time. For $T$-dependent measurements in a magnetic field of $H = 0$ or 6 T, the sample was cooled down from 90 K ($> T_N$) in an electric field $E_{\mathrm{poling}}$ larger than 0.08 MV/m and a corresponding magnetic field $H$. Magnetic field of 6 T is below the critical field of 6.4 T for the spin-flop transition at 55 K [19]. Optical absorption measurements were carried out in a cryostat equipped with a 15-T magnet at High Field Laboratory for Superconducting Materials in Tohoku University. A crystal of $MnTiO_3$ was shaped into a plate with large $c$ planes and polished to reduce the thickness $d$ to 90 $\mu$m. Gold with a thickness of 250 Å was sputtered onto both $c$ planes to form electrodes. Optical absorption spectra were measured by a spectrometer equipped with a CCD detector.

We first investigate the in-plane components $a_t$ and $a_\perp$ of ME effects, which are still unveiled experimentally. Magnetically induced electric polarization in $MnTiO_3$ is shown in Fig. 2(a). The presence of magnetically induced in-plane polarization below $T_N$ is apparent. The value of ME susceptibilities is estimated to be $a_\perp = 0.1$ and $a_t = 0.7$ ps/m at 55 K, which are smaller than $a_\parallel = 3.2$ ps/m. In addition, temperature dependence of $a_t$ and $a_\perp$ is different from $a_\parallel$, reflecting uniaxial magnetic anisotropy [16]. The former grows monotonically with cooling, while the latter takes its maximum at 53 K. The ME response is similar to that in $Cr_2O_3$ except for the presence of $a_t$, which is essential for directional dichroism.

The linear relationship between electric polarization $P_c$ along the $c$ axis and $H_c$ is displayed in Fig. 2(b), which qualitatively agrees with the previous report [18]. The coupling constant $a_\parallel$ changes its sign according to the signs of the poling electric and magnetic fields. The sign reversal of $a_\parallel$ indicates the switching of staggered moments $\boldsymbol{L}$ and hence the toroidal moment $\boldsymbol{T}$. Figure 2(c) shows the $P_c - E_c$ hysteresis loop of magnetically induced $P_c$ at 6 T, 55 K. The residual polarization of $\sim 15\ \mu\mathrm{C/m^2}$ in Fig. 2(c) is consistent with the polarization induced by $H_c$ of 6 T, as shown in Fig. 2(b). It is clearly shown that an electric field of 0.25 MV/m isothermally switches the magnetically induced polarization at 55 K, 6 T. The magnitude of the coercive electric field for $MnTiO_3$ is comparable to that for $Cr_2O_3$ [20]. Considering the coupling between the sign of $a_\parallel$, the staggered moments $L_c$, and the toroidal moment $T^c$, it is revealed that $T^c$ in $MnTiO_3$ should be isothermally switchable by a combination of $E_c$ and $H_c$.

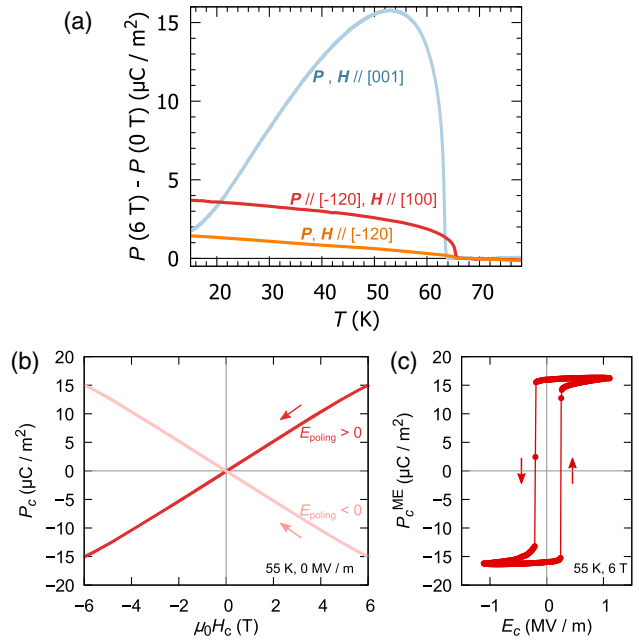


FIG. 2. (a) Magnetically induced electric polarization $P$ in $MnTiO_3$ in the absence of electric field in a temperature $T$-increasing run. (b) Magnetic-field dependence of $P$ in $MnTiO_3$. Before each measurement, an electric field $E_{\mathrm{poling}}$ of $\pm 1.1$ MV/m and a magnetic field of 6 T were applied along the $c$ axis at 55 K and then the electric field was switched off. (c) Electric-field dependence of magnetically induced component of $P$ in $MnTiO_3$ in a magnetic field of 6 T along the $c$ axis. Component in $P$ induced by the external electric field is subtracted.

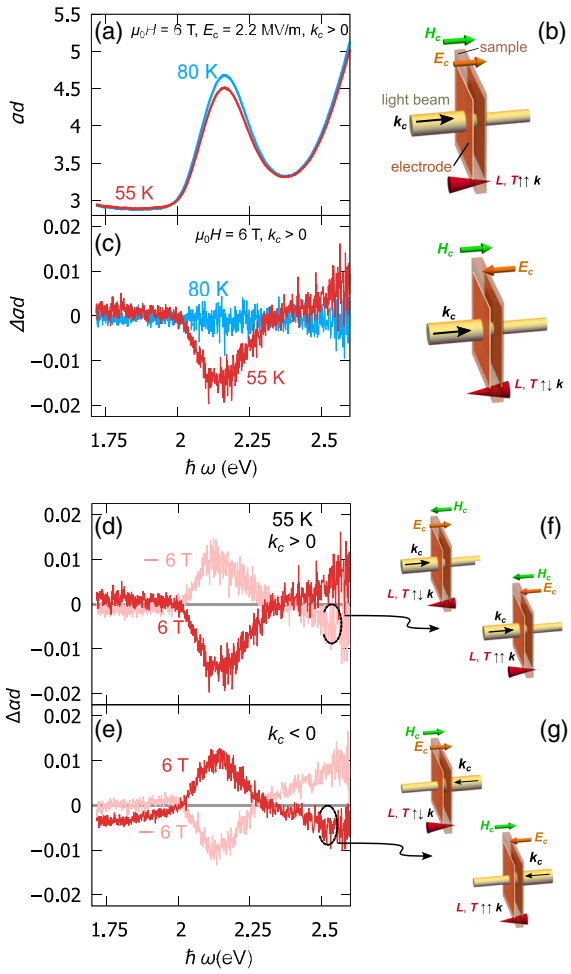


FIG. 3. (a) Optical absorption spectra of $MnTiO_3$ at 55 and 80 K in a magnetic field of $\mu_0 H_c = 6$ T and an electric field of $E_c = 2.2$ MV/m. (b) Experimental configuration of the measurements of the differential spectrum for the light propagating along the $c$ axis. External electric and magnetic fields are simultaneously applied along the $c$ axis. The electric field is isothermally switched between $E_c = 2.2$ and $-2.2$ MV/m to reverse the direction of $\boldsymbol{L}$. (c) Differential spectra $\Delta\alpha d(\omega)$ of $MnTiO_3$ between an electric field $E_c = 2.2$ and $-2.2$ MV/m. The contribution of the scattering by the gold electrodes to the observed electrochromic effect is also excluded. (d),(e) The variation of $\Delta\alpha d(\omega)$ with the reversal of magnetic field and/or the direction of light propagation. (f),(g) Experimental configurations corresponding to (d) and (e), respectively. Compared with (b), the magnetic field $\boldsymbol{H}$ is reversed in (f) and the propagation vector $\boldsymbol{k}$ is reversed in (g).

In order to verify the directional dichroism in $MnTiO_3$, we investigate the difference in absorption spectra between $\boldsymbol{L}, \boldsymbol{T}\uparrow\uparrow\boldsymbol{k}$ and $\boldsymbol{L}, \boldsymbol{T}\uparrow\downarrow\boldsymbol{k}$ [1]. The absorption spectra of $MnTiO_3$ for unpolarized light propagating along the $c$ axis parallel to the magnetic field of $\mu_0 H_c = 6$ T at 80 ($> T_N$) and 55 K ($< T_N$) is shown in Fig. 3(a). Two absorption bands are observed; a peak in the spectrum around 2.15 eV and the monotonic increase in $\alpha d$ above 2.4 eV [19]. The former one is assigned to an intra-atomic $d-d$ excitation from the ${}^6A_{1g}$ ground state to the ${}^4T_{1g}$ excited state of octahedrally coordinated $Mn^{2+}$ with $d^5$ electrons. The latter would be ascribed to the excitation to the ${}^4T_{2g}$ excited state overlapped with the charge transfer excitation [19] from O $2p$ to Mn $3d$.

For the investigation of the differential spectra, we first switch the direction of $\boldsymbol{L}$ with keeping $\boldsymbol{k}$ fixed. The sign of $L_c$ is reversed with the reversal of $E_c$ of $\pm 2.2$ MV/m in $\mu_0 H_c = 6$ T [Fig. 3(b)]. As shown in Fig. 2(c), $E_c$ of 2.2 MV/m is large enough to switch $T^c$ in a magnetic field of $\mu_0 H_c = 6$ T. Figure 3(c) shows spectra of differential absorption $\Delta\alpha d = \alpha d(E_c > 0) - \alpha d(E_c < 0)$ at 55 and at 80 K. The difference in absorption around 2.15 eV only emerges at 55 K $< T_N$, indicating that the antiferromagnetic ordering is essential to the electric-field induced suppression of absorption $\alpha$.

The sign of $\alpha^{E1-M1}(\omega)$ in Eq. (1) should depend on whether the light propagation vector $\boldsymbol{k}$ is parallel or antiparallel to toroidal moment $\boldsymbol{T}$ [5]. Figures 3(d) and 3(e) show variation of the differential spectrum with the reversal of $\boldsymbol{H}$ or $\boldsymbol{k}$. The corresponding experimental situation is schematically shown in Figs. 3(f) and 3(g). The electrochromic effect changes its sign with the reversal of $\boldsymbol{H}$ [Fig. 3(d)] or $\boldsymbol{k}$ [Fig. 3(e)], which agrees with the expected feature of

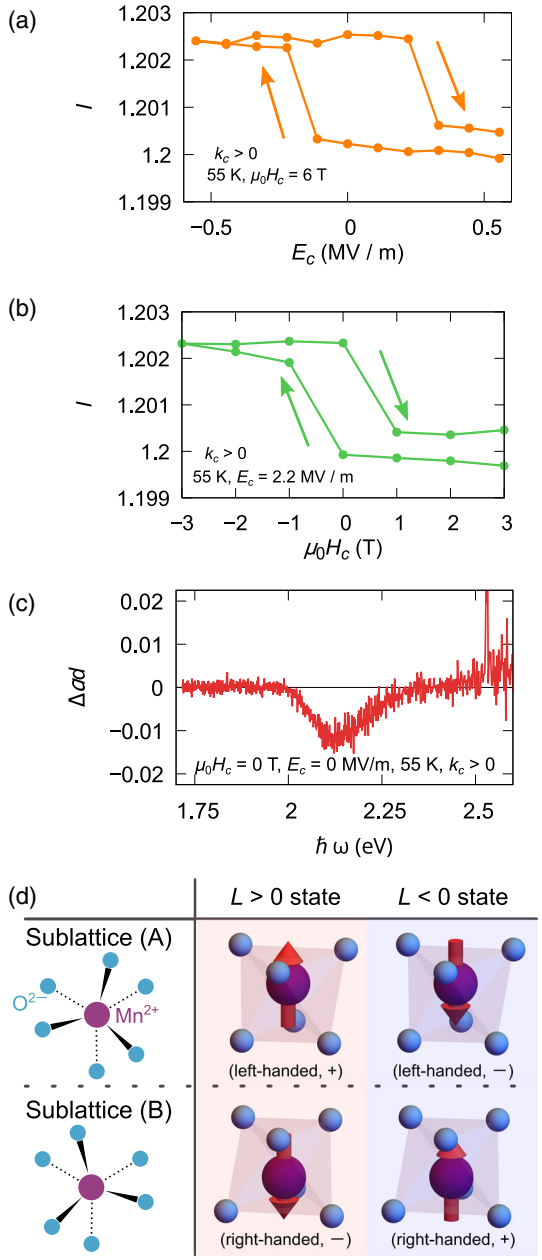


FIG. 4. (a) Control of absorbance in $MnTiO_3$ by sweeping (a) electric and (b) magnetic fields. The integrated absorption intensities $I = \int_{2.0\ \mathrm{eV}}^{2.3\ \mathrm{eV}} \alpha d d(\hbar\omega)$ for a photon-energy range between 2.0 and 2.3 eV are plotted. (c) Differential spectra of $MnTiO_3$ in the absence of external fields between two different antiferromagnetic states. (d) Relation among the coordination environment, local magnetization, and the sign of MCHD of each $MnO_6$ cluster. Pairs of two $MnO_6$ clusters with the same sign of $T^c$ and MCHD are shaded with the same color, red or blue according to the chirality (left or right handed) and local magnetization (+) or (−). Purple and blue spheres are $Mn^{2+}$ and $O^{2-}$ ions, respectively. Arrows on $Mn^{2+}$ ions denote magnetic moments. Schematic top view of each $MnO_6$ cluster is shown in the left column.

directional dichroism of $\boldsymbol{T}$ origin. The sign of the product of electric and magnetic fields determines the orientation of $\boldsymbol{T}$. The state of $T^c > 0$ is realized in the condition of $E_c > 0$ and $H_c > 0$, as well as $E_c < 0$ and $H_c < 0$, while the state of $T^c < 0$ appears if the signs of $E_c$ and $H_c$ are opposite of each other. The electrochromic effect should hence be $\boldsymbol{H}$ odd. The $\boldsymbol{k}$-odd nature of the electrochromic effect at 6 and −6 T shown in Fig. 3(g) also agrees with the $E1$–$M1$ interference. We conclude that the electrochromic effect observed in $MnTiO_3$ is assigned to directional dichroism of $\boldsymbol{T}$ origin.

Figure 4(a) demonstrates the binary switching in absorption by the isothermal cyclic reversal of electric voltage. The coercive electric field to switch the absorption is around 0.25 MV/m when $\mu_0 H_c = 6$ T, comparable with that in the $P_c - E_c$ loop [Fig. 2(b)]. The absorption is also switchable by sweeping $H_c$ in a steady electric field, as shown in Fig. 4(b). The hysteresis loops of $\alpha$ with some residual absorption indicate that the dichroism should appear without electric or magnetic field. Considering Eq. (3), the switching of $L_c$ and $T^c$ takes place when the product of $E_c$ and $H_c$ reaches the threshold value [21]. From this aspect, the coercive fields in the hysteresis loops of $\alpha$ for electric- [Fig. 4(a)] and magnetic-field sweep [Fig. 4(b)] are consistent with each other. In both cases, the critical value of the product $E_c H_c$ for the switching of $\alpha$ is approximately 1 TW/m$^2$, which corresponds to ME free energy of 1 neV/f.u. in Eq. (3).

To confirm that the observed dichroism is not induced by external fields but is a spontaneous effect, we focus on the absorption coefficient in the absence of both magnetic and electric fields. Figure 4(c) shows the differential spectra $\Delta\alpha d = (\alpha_+ - \alpha_-)d$ in the absence of external fields. $\alpha_+$ ($\alpha_-$) represents the absorption coefficient after poled by $E_c = 2.2$ MV/m and $\mu_0 H_c = 1\,(-1)$ T. The dip around 2.15 eV in Fig. 4(c) shows that the dichroism in $MnTiO_3$ of staggered moment $L_c$ origin is a spontaneous effect that occurs without net magnetization, in sharp contrast to the cases of conventional MCHD.

Finally, we discuss the microscopic origin of the directional dichroism in $MnTiO_3$ in terms of MCHD. Buckled honeycomb layers consist of two distinct sublattices. There are two kinds of orientations of $MnO_6$ clusters depending on which sublattice they are on [Fig. 4(d)]. Each $MnO_6$ cluster has the chiral $C_3$ symmetry. Since two types of $MnO_6$ are connected with the spatial-inversion operation, they have opposite handedness to each other. In the antiferromagnetic phase, each $MnO_6$ cluster with an ordered magnetic moment along the $c$ axis can be viewed as a magnetized chiral object. Furthermore, the direction of magnetic moment on each $MnO_6$ cluster also depends on the sublattice [Fig. 4(d)], when the sign of $L$ is fixed. In magnetized chiral objects, the sign of the MCHD is determined by the direction of the toroidal moment, which

is derived from the product of chirality and magnetization. Therefore, all the $MnO_6$ clusters host $T^c$ of the same sign and constructively contribute to the MCHD. In this way, antiferromagnetic ordering spontaneously induces MCHD in intrinsically racemic $MnTiO_3$, which switches its sign with the reversal of $T^c$.

This work was partly supported by JSPS KAKENHI Grants No. 16K13828, No. 16H01065, No. 17H02917, No. 18H04309, No. 19H01835, and No. JP19H05826. The x-ray diffraction and measurement of electric polarization were performed using facilities at the Institute for Solid State Physics, the University of Tokyo. Optical measurements in high magnetic fields were performed at the High Field Laboratory for Superconducting Materials, Institute for Material Research, Tohoku University (Project No. 19H0050). T. S. is supported by JSPS through Program for Leading Graduate Schools (MERIT).

[1] G. L. J. A. Rikken and E. Raupach, Phys. Rev. E **58**, 5081 (1998).
[2] N. Baranova, Y. V. Bogdanov, and B. Y. Zel'Dovich, Opt. Commun. **22**, 243 (1977).
[3] G. Wagnière and A. Meier, Chem. Phys. Lett. **93**, 78 (1982).
[4] L. Barron and J. Vrbancich, Mol. Phys. **51**, 715 (1984).
[5] L. D. Barron, *Molecular Light Scattering and Optical Activity* (Cambridge University Press, Cambridge, England, 2009).
[6] V. Dubovik and V. Tugushev, Phys. Rep. **187**, 145 (1990).
[7] C. Train, R. Gheorghe, V. Krstic, L.-M. Chamoreau, N. S. Ovanesyan, G. L. Rikken, M. Gruselle, and M. Verdaguer, Nat. Mater. **7**, 729 (2008).
[8] M. Saito, K. Ishikawa, K. Taniguchi, and T. Arima, Phys. Rev. Lett. **101**, 117402 (2008).
[9] N. Nakagawa, N. Abe, S. Toyoda, S. Kimura, J. Zaccaro, I. Gautier-Luneau, D. Luneau, Y. Kousaka, A. Sera, M. Sera *et al.*, Phys. Rev. B **96**, 121102(R) (2017).
[10] V. Baltz, A. Manchon, M. Tsoi, T. Moriyama, T. Ono, and Y. Tserkovnyak, Rev. Mod. Phys. **90**, 015005 (2018).
[11] T. Jungwirth, X. Marti, P. Wadley, and J. Wunderlich, Nat. Nanotechnol. **11**, 231 (2016).
[12] P. Němec, M. Fiebig, T. Kampfrath, and A. V. Kimel, Nat. Phys. **14**, 229 (2018).
[13] V. Kocsis, K. Penc, T. Rõõm, U. Nagel, J. Vit, J. Romhányi, Y. Tokunaga, Y. Taguchi, Y. Tokura, I. Kézsmárki *et al.*, Phys. Rev. Lett. **121**, 057601 (2018).
[14] K. Kidoh, K. Tanaka, F. Marumo, and H. Takei, Acta Crystallogr. Sect. B **40**, 329 (1984).
[15] G. Shirane, S. Pickart, and Y. Ishikawa, J. Phys. Soc. Jpn. **14**, 1352 (1959).
[16] H. Yamauchi, H. Hiroyoshi, M. Yamada, H. Watanabe, and H. Takei, J. Magn. Magn. Mater. **31**–**34**, 1071 (1983).
[17] I. E. Dzyaloshinskii, Sov. Phys. JETP **10**, 628 (1960).
[18] N. Mufti, G. R. Blake, M. Mostovoy, S. Riyadi, A. A. Nugroho, and T. T. M. Palstra, Phys. Rev. B **83**, 104416 (2011).
[19] J. G. Cherian, T. D. Tokumoto, H. Zhou, E. S. Choi, and S. A. McGill, Phys. Rev. B **87**, 214411 (2013).
[20] A. Iyama and T. Kimura, Phys. Rev. B **87**, 180408(R) (2013).
[21] T. V. A. Nguyen, Y. Shiratsuchi, A. Kobane, S. Yoshida, and R. Nakatani, J. Appl. Phys. **122**, 073905 (2017).